Sulfatides are required for renal adaptation to chronic metabolic acidosis

Paula Stettner[a], Soline Bourgeois[b], Christian Marsching[c,d,e], Milena Traykova-Brauch[a], Stefan Porubsky[a], Viola Nordström[a], Carsten Hopf[d,e], Robert Koesters[f], Roger Sandhoff[c,d,e], Herbert Wiegandt[a], Carsten A. Wagner[b], Hermann-Josef Gröne[a,e,1], and Richard Jennemann[a,1]

[a]Department of Cellular and Molecular Pathology, German Cancer Research Center, D-69120 Heidelberg, Germany; [b]Institute of Physiology and Center for Integrative Human Physiology, University of Zurich, CH-8057 Zurich, Switzerland; [c]Lipid Pathobiochemistry Group, Department of Cellular and Molecular Pathology, German Cancer Research Center, D-69120 Heidelberg, Germany; [d]Institute of Instrumental Analytics and Bioanalytics, Department of Biotechnology, University of Applied Sciences, D-68163 Mannheim, Germany; [e]Center for Applied Biomedical Mass Spectrometry, D-68163 Mannheim, Germany; and [f]Hopital Tenon, Unité Mixte de Recherche S 702, Institut National de la Santé et de la Recherche Médicale/University of Paris 6, 75020 Paris, France

Edited* by Sen-itiroh Hakomori, Pacific Northwest Research Institute, Seattle, WA, and approved May 1, 2013 (received for review October 16, 2012)

Urinary ammonium excretion by the kidney is essential for renal excretion of sufficient amounts of protons and to maintain stable blood pH. Ammonium secretion by the collecting duct epithelia accounts for the majority of urinary ammonium; it is driven by an interstitium-to-lumen NH_3 gradient due to the accumulation of ammonium in the medullary and papillary interstitium. Here, we demonstrate that sulfatides, highly charged anionic glycosphingolipids, are important for maintaining high papillary ammonium concentration and increased urinary acid elimination during metabolic acidosis. We disrupted sulfatide synthesis by a genetic approach along the entire renal tubule. Renal sulfatide-deficient mice had lower urinary pH accompanied by lower ammonium excretion. Upon acid diet, they showed impaired ammonuria, decreased ammonium accumulation in the papilla, and chronic hyperchloremic metabolic acidosis. Expression levels of ammoniagenic enzymes and Na^+-K^+/NH_4^+-$2Cl^-$ cotransporter 2 were higher, and transepithelial NH_3 transport, examined by in vitro microperfusion of cortical and outer medullary collecting ducts, was unaffected in mutant mice. We therefore suggest that sulfatides act as counterions for interstitial ammonium facilitating its retention in the papilla. This study points to a seminal role of sulfatides in renal ammonium handling, urinary acidification, and acid–base homeostasis.

Low blood pH, as it occurs in metabolic acidosis, affects cellular functions and can lead to increased morbidity and mortality (1). The mammalian kidney plays a central role in the regulation of extracellular osmolality and fluid volume as well as the maintenance of blood pH in a narrow range of pH 7.35–7.45 (2). Excess protons are buffered by bicarbonate synthesized during renal ammoniagenesis and excreted into urine mainly bound to NH_4^+ (ammonium) and titratable acids. During metabolic acidosis, enhanced ammonium excretion accounts for more than 80% of the increase in urinary net acid excretion in humans and rodents (3, 4). Ammonium (NH_3 and NH_4^+) is produced in proximal tubular (PT) epithelia, secreted into the PT lumen, and is largely reabsorbed in the thick ascending limb of Henle's loop (TAL). This process results in high interstitial ammonium concentrations in the medulla and the papilla and thereby, in parallel to the gradient of hypertonicity, in a corticopapillary ammonium gradient facilitating secretion of ammonium into medullary collecting ducts (4). Several transport proteins have been shown to mediate medullary TAL NH_4^+ reabsorption (5). However, the mechanisms that underlie the maintenance of high interstitial NH_4^+ concentrations in the medulla and papilla, thereby avoiding backflux into the systemic circulation, have remained unexplored.

Sulfatides are a subclass of anionic glycosphingolipids (GSLs), which consist of ceramide and carbohydrate residues to which one or several sulfate esters are bound via enzymatic catalysis by cerebroside sulfotransferases (CST; *Cst*). In mammals, sulfatides accumulate in the kidney with particularly high concentrations in the distal nephron segments and the renal medulla (6). The major renal sulfatide in humans and rodents is the galactosylceramide (GalCer)-derived SM4s. Other sulfated GSL species such as the glucosylceramide (GlcCer)-derived SM3 (sulfated lactosylceramide) in humans and mice and SB1a (gangliotetraosylceramide-bis-sulfate) in mice are even more polar than SM4s (7) (Fig. 1*A*).

Various kidney diseases such as renal cell carcinoma and polycystic kidney disease are associated with disturbances in renal sulfatide metabolism (8, 9). However, the basic physiological function of renal sulfatides is not known. They are mainly found in the outer part of the plasma membrane. Apart from mediating cellular interactions with various external ligands, e.g., L-selectin, the anionic charge carried by sulfatides on the membrane surface may point to a modulatory role in membrane ion fluxes and/or binding of cationic extracellular substrates (7, 10, 11). Sulfatides at the cell membrane were surmised to function as ion barriers to extracellular osmolality oscillation (12, 13). Furthermore, they have been discussed to act as cofactors of basolateral Na^+-K^+-ATPase activity by binding K^+ or by facilitating the membrane relocalization of the enzyme (14–16). Zalc et al. (17) have proposed a role of sulfatides rather in passive sodium chloride diffusion in the TAL.

However, renal abnormalities have not been reported either in mice with systemic disruption of UDP-galactose:ceramide galactosyltransferase (*Cgt*; CGT) lacking SM4s or in $Cst^{-/-}$ mice with deficiency of all sulfatides most probably due to the dominant and finally lethal central nervous system phenotypes (18, 19).

The aim of this study was to assess in vivo the hypothesis that sulfatides are involved in ion transport processes in the kidney by a combined molecular genetic and physiological approach. Therefore, we have generated mice with disruption of the *Cst* gene and UDP-glucose:ceramide glucosyltransferase (*Ugcg*) gene and combinations of both in a tubular epithelial cell-specific manner under control of the paired box gene 8 (Pax8) promoter (20). This approach was taken to reduce the possibility for compensatory synthesis of charged GSLs as well as to circumvent systemic effects (18, 21, 22). Here, we show that sulfatides, most probably by their anionic extracellular charge, are required to maintain high interstitial ammonium concentration in the papilla, which is needed for

Author contributions: P.S., S.B., C.M., H.W., C.A.W., H.-J.G., and R.J. designed research; P.S., S.B., C.M., M.T.-B., S.P., V.N., R.S., H.-J.G., and R.J. performed research; C.H. and R.K. contributed new reagents/analytic tools; P.S., S.B., C.M., and R.J. analyzed data; and P.S., C.A.W., H.-J.G., and R.J. wrote the paper.

The authors declare no conflict of interest.

Glycosphingolipids are abbreviated according to the recommendations of the UPAC-International Union of Biochemistry Joint Commission (J Mol Biol. 1999;286:963-70).

*This Direct Submission article had a prearranged editor.

[1]To whom correspondence may be addressed. E-mail: r.jennemann@dkfz.de or h.-j.groene@dkfz-heidelberg.de.

This article contains supporting information online at www.pnas.org/lookup/suppl/doi:10.1073/pnas.1217775110/-/DCSupplemental.

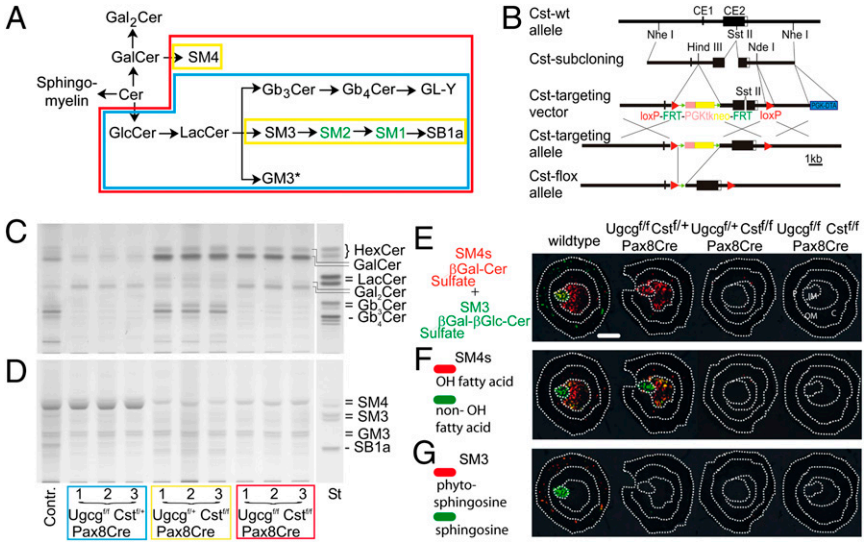

Fig. 1. Pax8-driven deletion of renal neutral and sulfated GSLs. (*A*) *Ugcg*- and *Cst*-dependent synthesis of neutral and acidic GSLs in the mouse kidney. (*B*) Cloning strategy for the disruption of the *Cst* gene. Disruption of the *Ugcg* gene has been described previously (47). (*C* and *D*) Neutral (*C*) and acidic (*D*) GSL extracts from one control mouse and $Ugcg^{f/f}$, $Cst^{f/f}$, and $Ugcg^{f/f}$ $Cst^{f/f}$ Pax8Cre mice ($n = 3$ each) were separated by TLC. Aliquots from extracts corresponding to 4 mg of dry weight of kidneys were loaded. Pronounced reduction of *both* GlcCer-based and all sulfated GSLs (SM4s, SM3, and SB1a) was found in kidneys from $Ugcg^{f/f}$ $Cst^{f/f}$ Pax8Cre mice only. *GM3 ganglioside is obviously expressed in other cell types (endothelial, stromal) than those that express the Pax8Cre recombinase and remains therefore unaltered in mutant kidney (*A* and *D*). (*E*–*G*) MALDI-MSI of renal sulfatides in control mice and mice with kidney-specific sulfatide deficiency. (*E*) The sum of all detected isoforms of SM4s (red) and complex SM3 (green) that overlap in the papilla. (*F*) SM4s isoforms with hydroxylation in the inner medulla (red) are mainly detected in the inner medulla, whereas more lipophilic isoforms without this modification (green) are mainly detected in the papillary region. (*G*) Complex SM3 without any modification in the ceramide anchor (green) shows a specific location to the papilla, whereas more hydrophilic isoforms with a hydration of the double bond of the sphingoid base (red) are located to the renal cortex. (Scale bar, 1 mm.) C, cortex; IM, inner medulla; OM, outer medulla; P, papilla. Each section shown is representative of $n = 3$ mice per genotype.

appropriate ammonium excretion into urine under basal conditions and during metabolic acidosis.

Results

Cell-Specific Depletion of GlcCer-Derived and Sulfated GSLs in Mouse Kidney. $Ugcg^{f/f}$ $Cst^{f/f}$ Pax8Cre and respective single-enzyme mutant mice were born according to Mendelian inheritance. Southern blot analysis showed cell-specific disruption of the *Ugcg* and *Cst* genes in kidney as expected from the activity of the Pax8 promoter (*SI Appendix*, Fig. S1 *A*–*G*). Deletion of the gene products was verified by TLC of neutral and acidic GSLs extracted from mutant mice kidneys (Fig. 1 *C* and *D* and *SI Appendix*, Fig. S1*I*). In $Ugcg^{f/f}$ $Cst^{f/+}$ Pax8Cre kidneys, GlcCer-dependent neutral and acidic GSLs were strongly decreased compared with controls as evident from bands corresponding to the globoseries (Fig. 1*C*) and complex sulfatides (SM3, SB1a), whereas SM4s remained unaltered (Fig. 1*D* and *SI Appendix*, Fig. S1*I*). In contrast, in kidneys from $Ugcg^{f/+}$ $Cst^{f/f}$ and $Ugcg^{f/f}$ $Cst^{f/f}$ Pax8Cre mice, all sulfated GSL species could be detected in only minute amounts. Remnant traces of SM4s were possibly due to cells in which Cre recombinase was not active (Fig. 1*D* and *SI Appendix*, Fig. S1*I*). Single disruption of *Cst* did not affect the synthesis of renal neutral GSLs. The strong band at the height of monohexosylceramide detected in kidneys with *Cst* deficiency ($Ugcg^{f/+}$ $Cst^{f/f}$ and $Ugcg^{f/f}$ $Cst^{f/f}$ Pax8Cre kidneys) was due to an accumulation of GalCer, as reported previously (7). In addition, Gal_2Cer (at the height of dihexosylceramide) increased in kidneys with *Ugcg* deficiency ($Ugcg^{f/f}$ $Cst^{f/+}$ and $Ugcg^{f/f}$ $Cst^{f/f}$ Pax8Cre kidneys) (Fig. 1*C*). In line, no shift to sphingomyelin was seen in any of the mutant mice kidneys (*SI Appendix*, Fig. S1*H*).

The compartment-specific distribution of sulfatide species and isoforms and their deficiency in mutant mice was further demonstrated on mouse kidney sections by applying MALDI mass-spectrometric imaging (MSI) (Fig. 1 *E*–*G*). Both, TLC of acidic GSL extracts from cortical, medullary, and papillary tissue from wild-type mice, as well as MSI revealed that SM4s and SM3 were concentrated in the papilla (Fig. 1 *E*–*G* and *SI Appendix*, Fig. S1*J*).

Lack of Renal Sulfatides Leads to More Acidic Urinary pH. Renal *Ugcg*/*Cst* and respective single-enzyme–deficient mice had a normal life span. Kidney morphology appeared regular by light microscopy and transmission electron microscopy (*SI Appendix*, Fig. S2). Creatinine clearance was similar compared with control littermates (*SI Appendix*, Table S1). However, all mutant mouse groups had a significantly lower urinary pH (Fig. 2*A*). Notably, urine of renal *Cst*- and *Ugcg*/*Cst*-deficient mice was more acidic compared with that of renal *Ugcg*-deficient animals, indicating the major role of sulfatides in urinary pH regulation (Fig. 2*A*). Additionally, mice with *Cst* and *Ugcg*/*Cst* deficiency had lower ammonium excretion (Fig. 2*B*) as well as higher urinary potassium and urinary output (*SI Appendix*, Table S1).

Induction of Metabolic Acidosis in Renal *Ugcg*/*Cst*-Deficient Mice. Despite the significantly lower urinary pH and reduced ammonium excretion, blood pH and bicarbonate levels in renal *Ugcg*/*Cst*–double-deficient mice were in the physiological range under control diet suggesting compensatory mechanisms for altered renal acid–base handling. In fact, urinary excretion of titratable acids (TAs) in mutant mice was significantly higher compared with controls (*SI Appendix*, Table S1). Foremost renal *Ugcg*/*Cst*

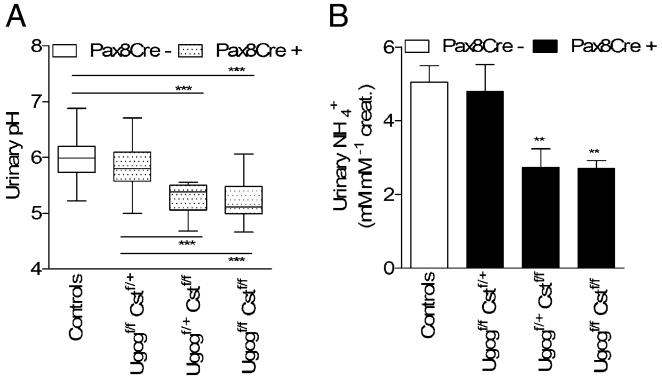

Fig. 2. Renal deficiency of sulfatides induced a urinary pH and ammonium excretion lower than in sulfatide-expressing kidney. Urinary pH and ammonium of renal *Ugcg*-, *Cst*-, and *Ugcg*/*Cst*-deficient mice is shown compared with their respective control littermates. (*A*) $n = 58$ in controls, $n = 26$ in $Ugcg^{f/f}$ Pax8Cre, $n = 14$ in $Cst^{f/f}$ Pax8Cre, and $n = 19$ in $Ugcg^{f/f}$ $Cst^{f/f}$ Pax8Cre mice. (*B*) $n = 19$ in controls, $n = 7$ in $Ugcg^{f/f}$ Pax8Cre, $n = 8$ in $Cst^{f/f}$ Pax8Cre, and $n = 9$ in $Ugcg^{f/f}$ $Cst^{f/f}$ Pax8Cre mice. Means ± SEM are shown (**$P < 0.01$; ***$P < 0.001$).

PHYSIOLOGY

double-enzyme–deleted mice with no ability to compensate for the lack of sulfatides by de novo synthesis of *Ugcg*-derived anionic GSLs were chosen to study further the influence of sulfatide deficiency on renal handling of an acid challenge. In addition, single mutant mice were exposed to a chronic acid load.

Mutant mice and respective control littermates were exposed to an acute (2 d) and chronic (9 d) hydrochloric acid (HCl) diet. The acute HCl load induced a significant decrease in blood pH and bicarbonate levels and an increase in blood chloride levels in both groups *Ugcg*/*Cst*–double-deficient mice and controls (Fig. 3 *A*–*C*). Control mice adapted well by a strong increase in ammonium excretion and partially recovered by day 9 their blood pH and bicarbonate (Fig. 3 *A*–*C* and *E*). *Ugcg*/*Cst*-deficient mice, however, showed a reduced capacity (−30%) to increase their ammonuria resulting in less net acid excretion (NAE) than controls (Fig. 3 *E* and *F*). Urinary pH in control mice declined significantly upon acute acid loading followed by a recovery during chronic acid challenge, whereas renal *Ugcg*/*Cst*-deficient mice maintained their low pH throughout the 9-d experimental period (Fig. 3*D*). The urinary phenotype in *Ugcg*/*Cst*-deficient mice was paralleled by chronic hyperchloremic metabolic acidosis as indicated by more acidic blood pH, lower blood bicarbonate, and decreased body weight compared with control mice (Fig. 3 *A*–*C*, *SI Appendix*, Fig. S3, and *SI Appendix*, Table S2). To exclude the possibility of involvement of neutral and other acidic glycosphingolipids, blood pH, bicarbonate, and chloride as well as urinary pH and ammonuria was measured in parallel in single- and double-mutant mice after chronic acid loading. Consistent with significantly reduced ammonium excretion, only mice lacking renal *Cst* expression showed significantly increased metabolic acidosis compared with controls (*SI Appendix*, Fig. S4 *A*–*E*).

Reduced Papillary Ammonium Accumulation in Renal *Cst*- and *Ugcg*/*Cst*-Deficient Mice. Medullary TAL ammonium reabsorption and the associated cortico-papillary ammonium concentration gradient are enhanced during chronic acidosis (23, 24). To examine whether *Ugcg*/*Cst*-deficient mice are able to create such a gradient, we dissected cortical, medullary, and papillary parenchyma from kidneys of chronic acid-loaded mice. In the papilla, ammonium content was reduced by 30% in renal *Ugcg*/*Cst*-deficient kidneys. Medullary and cortical ammonium content did not significantly differ, although medullary ammonium content tended to be reduced. Renal *Ugcg*/*Cst*-deficient mice thus exhibited a significantly reduced cortico-papillary ammonium gradient compared with control littermates (Fig. 4*A*). In contrast, in mice with renal *Ugcg* deficiency, papillary ammonium content was not significantly changed compared with controls (Fig. 4*B*).

Expression and Activity of Ammoniagenic Enzymes and Ammonium Transporters in Renal *Ugcg*/*Cst*-Deficient Mice. Renal mRNA and protein levels, respectively, of the proximal tubular glutamine transporter sodium-coupled neutral amino acid transporter (SNAT3) and of ammoniagenic enzymes such as kidney-specific glutaminase and phosphoenolpyruvate carboxykinase (PEPCK) slightly increased in mutant vs. controls (Fig. 5 *A*–*C*, *G*, and *H*). The phosphate-dependent renal glutaminase activity was not significantly changed (*SI Appendix*, Fig. S4*F*). In addition, ammoniagenesis in isolated cortical proximal tubules from double-mutant mice was similar to controls (*SI Appendix*, Fig. S4*G*). Ammonium produced is secreted at least in part via the brush border membrane-localized Na^+-H^+/NH_4^+ exchanger-3 (NHE-3) into the lumen (25). NHE-3 mRNA levels in kidneys of renal *Ugcg*/*Cst*-deficient and control mice were similar (*SI Appendix*, Fig. S5*A*). In line, total NHE activity in isolated brush border membrane vesicles of *Ugcg*/*Cst*-deficient kidneys was unaffected, as revealed by using the acridine orange quenching method (*SI Appendix*, Fig. S5*B*). mRNA and protein expression, respectively, of transporters involved in TAL ammonium reabsorption such as the apical Na^+-K^+/NH_4^+-$2Cl^-$ cotransporter 2 (NKCC2), basolateral Na^+/NH_4^+-H^+ exchanger 4 (NHE-4), as well as electroneutral Na^+-bicarbonate cotransporter 1 (NBCn1) were significantly increased or similar to controls in *Ugcg*/*Cst*-deficient kidneys (Fig. 5 *D*–*H*).

mRNA expression of major acid–base transporters in the collecting duct (CD) was not affected in renal *Ugcg*/*Cst*-deficient mice (*SI Appendix*, Fig. S6 *A*–*F*). The cellular activity of some of those transporters can be also regulated by their subcellular localization (26, 27). However, the cellular distribution of the V-ATPase subunits V1B1 (*SI Appendix*, Fig. S6 *G*–*J*), V0a4, and the major ammonium transporter rhesus blood group-associated C glycoprotein (Rhcg) (*SI Appendix*, Fig. S6 *K*–*N*) was not changed.

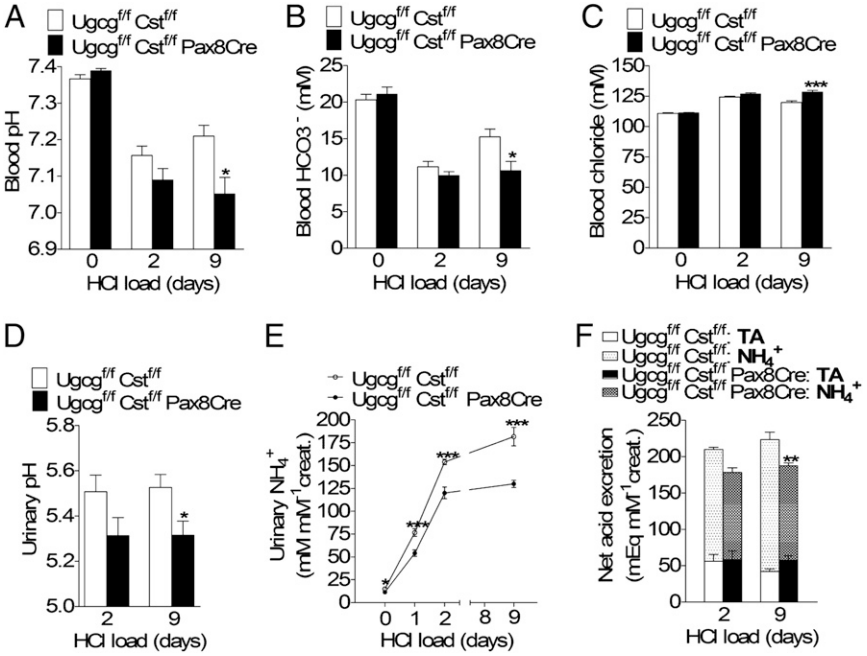

Fig. 3. Mice with lack of renal sulfatides show impaired acid stress handling. Renal *Ugcg*/*Cst*-deficient mice (n = 6–12) and control littermates (n = 8–14) were exposed to an oral acid challenge with hydrochloric acid (HCl). (*A*) Blood pH; (*B*) blood bicarbonate; (*C*) blood chloride; (*D*) urinary pH. (*E* and *F*) Reduced ammonuria (*E*) in response to acid loading in renal *Ugcg*/*Cst*-deficient mice resulted in reduced net acid excretion (*F*) compared with control mice. Excretion of titratable acidity (TA) (*F*) was not reduced in mutant mice. Means ± SEM are shown (*P < 0.05; **P < 0.01; ***P < 0.001).

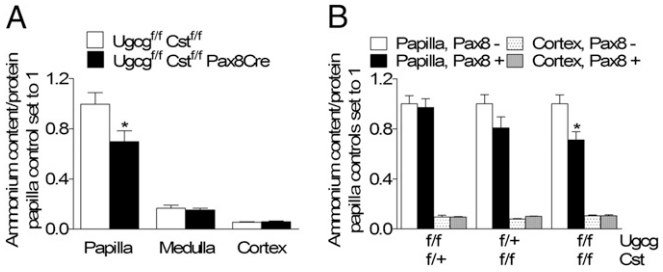

Fig. 4. Ammonium content in papilla of renal sulfatide-deficient mice was significantly reduced compared with controls. (*A*) Ammonium content in dissected cortical, medullary, and papillary kidney tissue from 9-d acid-loaded control and renal sulfatide-deficient mice was measured. $n = 8$ in controls and $n = 12$ in mutant mice. (*B*) Comparison of cortical and papillary ammonium content in *Ugcg*$^{f/f}$-deficient, *Cst*$^{f/f}$-deficient, and *Ugcg*$^{f/f}$ *Cst*$^{f/f}$–double-deficient mouse kidneys ($n = 5$–7 per group). Mean ± SEM is shown (*$P < 0.05$).

Unaltered Transepithelial NH_3 Transport in CDs from Renal *Ugcg*/*Cst*-Deficient Mice. The lack of sulfatides could possibly have influenced transporter-mediated or diffusive epithelial ammonium permeability or proton transport in the CD (4). We assessed this question by two different approaches. First, we measured apical NH_3, NH_4^+, and H^+ excretion by the NH_4Cl prepulse technique in in vitro-microperfused outer medullary CDs (OMCDs). The OMCD was chosen because it contains mostly acid-secretory type A intercalated cells but only very few bicarbonate-secretory type B intercalated cells. Second, we examined total transepithelial NH_3 permeability in the in vitro microperfused cortical CDs (CCDs) by imposing a bath-to-lumen NH_3 gradient in the nominal absence of an NH_4^+ gradient. Both approaches demonstrated that the capacity to transport NH_3 and protons was not altered by the renal lack of *Ugcg* and *Cst* (Fig. 6).

Decreased Aquaporin 2 Protein Levels in Renal *Ugcg*/*Cst*-Deficient Mice. Renal *Ugcg*/*Cst*-deficient mice showed higher urinary output and polydipsia under baseline and upon HCl loading (*SI Appendix*, Fig. S7 *A* and *B*). As renal sulfatides have been implicated in the urinary concentration process (10), we tested the ability of renal *Ugcg*/*Cst*-deficient mice to produce concentrated urine. Mice were exposed to an osmotic stress by water restriction for 24 h. Again, urine was less concentrated and urinary osmolality was lower in mutant mice (*SI Appendix*, Fig. S8 *A* and *B*). Plasma osmolality and renal osmotic gradient, as examined by measurement of tissue osmolality in separated cortical, outer medullary, and inner medullary tissue, were unaltered (*SI Appendix*, Fig. S8 *C* and *D*). In contrast, the expression of the aquaporin 2 (AQP2) water channel was significantly decreased compared with controls indicating reduced water reabsorption in CDs of renal *Ugcg*/*Cst*-deficient mice (*SI Appendix*, Fig. S8 *E* and *F*).

Discussion

Our study demonstrates that sulfatides influence urinary acidification; they are needed for acid–base homeostasis during acid loading.

Cell-specific genetic deletion of sulfatide synthesis was achieved by disruption of GSL-specific sulfotransferase while the possible compensatory synthesis of other negatively charged GSLs was inhibited by deletion of glucosylceramide synthase (*Ugcg*) activity.

Renal *Ugcg*-, *Cst*-, and *Ugcg*/*Cst*-deficient mice displayed lower urinary pH. By far more acidic urinary pH in renal *Cst*- and *Ugcg*/*Cst*-deficient compared with single *Ugcg*-deficient mice per se indicated the crucial role of sulfatides, in particular SM4s. In support of this, Gb3 synthase$^{-/-}$ mice with exclusive deficiency for neutral globo-series GSLs, another major component of renal GSLs, showed regular urinary pH (28).

The strongly lowered pH in *Cst*- and *Cst*/*Ugcg*-deficient mice was accompanied by lower ammonium excretion compared with control littermates. Lower urinary pH may be caused by a reduced capacity to buffer protons. Apparently, increased excretion of titratable acidity did not fully compensate for the lack of ammonium buffer in *Ugcg*/*Cst*-deficient mice. The lower amount of ammonium excretion is remarkable because it occurs in the presence of a steeper pH gradient. Nevertheless, acidic urine can increase the driving force for ammonium excretion, thereby partially compensating the defect in medullary ammonium accumulation and thereby partially rescuing the defect in ammonium excretion. By this mechanism, mice lacking the NHE-4 exchanger in the medullary TAL fully compensated deficient ammonium excretion at basic conditions (29).

Lower urinary pH in combination with higher NAE, but impaired use of ammonium buffer, has been described as a characteristic for patients with uric acid nephrolithiasis and was also found in patients with metabolic syndrome and type 2 diabetes (30, 31). The mechanisms underlying the dysfunctional renal ammonium excretion in humans with either of these diseases have not been explored so far (30). In Zucker diabetic fatty rats, ammoniagenesis and ammonium excretion by the PT may be affected (32).

Under standard diet, the reduced ammonium excretion (by about 4–5 $mM \cdot mM^{-1}$ creatinine) did not affect systemic acid–base homeostasis in renal *Cst*- and *Ugcg*/*Cst*-deficient mice. However, during an oral acid load, increased excretion of TA could not substitute for the ~30% reduction in urinary ammonium excretion. Renal *Cst*- and *Ugcg*/*Cst*-deficient mice developed hyperchloremic metabolic acidosis compared with controls; this phenomenon did not occur in renal *Ugcg*-deficient

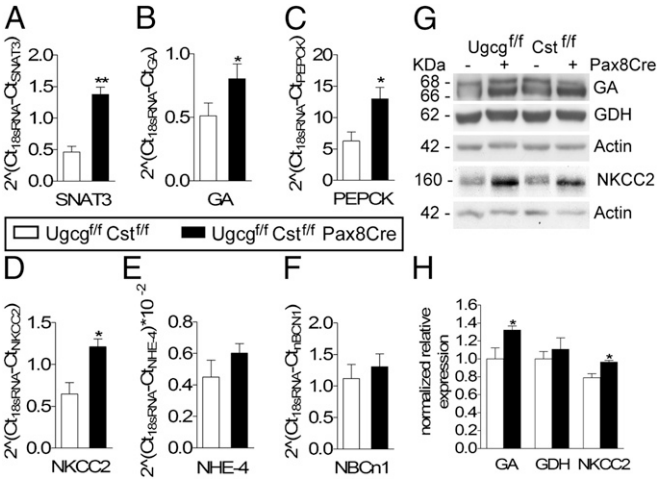

Fig. 5. Expression of enzymes and transporters relevant for ammonium production, TAL reabsorption, and delivery to the medullary interstitium. (*A*–*F*) Total mRNA was isolated from kidneys of 9-d acid-loaded control and renal *Ugcg*/*Cst*-deficient mice ($n = 5$ or 6 per genotype) and analyzed by real-time RT-PCR. (*A*) The sodium-coupled neutral amino acid transporter (SNAT3) and (*B*) the mitochondrial glutaminase (GA) involved in production of NH_4^+, as well as (*C*) the cytoplasmic phosphoenolpyruvate carboxykinase (PEPCK) mediating the generation of HCO_3^- and (*D*) the apical Na^+-K^+/NH_4^+-$2Cl^-$ cotransporter 2 (NKCC2) mediating net NH_4^+ reabsorption in the TAL were significantly increased in renal *Ugcg*/*Cst*-deficient kidneys. (*E*) The basolateral Na^+/NH_4^+-H^+ exchanger 4 (NHE-4) and (*F*) the electroneutral Na^+-bicarbonate cotransporter 1 (NBCn1) were elevated too, however not significantly. Means ± SEM are shown (*$P < 0.05$; **$P < 0.01$). (*G* and *H*) Western blot analysis of mitochondrial glutaminase (GA) and glutamate dehydrogenase (GDH), both involved in the production of NH_4^+, as well as the NKCC2 cotransporter in chronic acid-loaded mice. The cytoplasmic and membrane protein samples shown are representative of $n = 3$ in controls and $n = 5$ in mutant mice. Intensities of bands were densitometrically evaluated. Data are expressed as mean ± SEM (*$P < 0.05$).

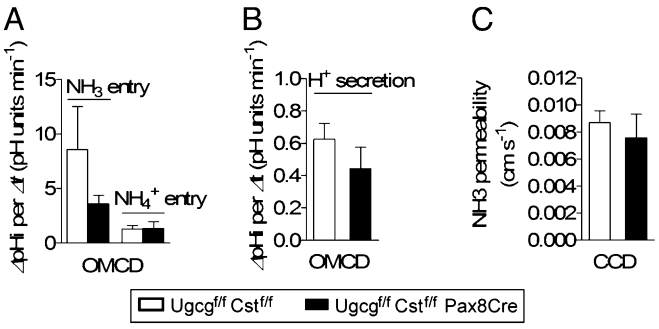

Fig. 6. Similar proton and ammonia transport activity in CDs segments from renal sulfatide-deficient mice. (*A*–*C*) In vitro microperfusion experiments of single isolated CCDs and OMCDs. (*A* and *B*) Transepithelial NH_3 and NH_4^+ inward (*A*) as well as proton outward movements (*B*) showed similar rates in intracellular alkalinization and pH recovery, suggesting unaltered luminal NH_3 entry and proton secretion by *Ugcg*/*Cst*-deficient OMCD intercalated cells. Means ± SEM are shown (n = 4 mice per genotype and n = 1–2 OMCDs per mouse). (*C*) Direct measurements of transepithelial NH_3 fluxes show unimpaired NH_3 permeability of *Ugcg*/*Cst*-deficient CCD epithelium. Means ± SEM are shown (n = 7 mice per genotype; n = 1 CCD per mouse).

mice with unaffected sulfatide SM4s expression. Consistent with impaired ammoniuria, acidotic mutant mice with complete sulfatide deficiency had significantly lower ammonium concentration selectively in the papilla compared with control mice. Notably, the phenotype of reduced ammonuria as well as deficient papillary ammonium content upon chronic acid loading was slightly less pronounced in single *Cst*-deficient mice compared with *Ugcg*/*Cst*-deficient mice. This could possibly be explained by the synthesis of an *Ugcg*-derived, sialylated GSL in single *Cst*-deficient mice (below the expected band of SB1a) (Fig. 1*D*), which may have exerted compensatory function for the lack of anionic sulfatides.

In contrast to other ions, ammonium is produced by the kidney itself and renal ammonium handling at baseline and during acidosis involves several nephron segments. Although the molecular mechanisms of renal ammonium transport are not completely elucidated, numerous proteins mediating NH_3 or NH_4^+ transport along the renal tubule have been identified so far (4). Despite the pronounced reduced urinary ammonium excretion, acidosis-induced renal *Ugcg*/*Cst*-deficient mice showed slightly enhanced expression of ammoniagenic enzymes and glutaminase activity to control mice. In addition, increased expression of NKCC2 was detected. Both changes in the PT and the TAL were apparently compensatory and very likely exclude the possibility of reduced ammonium delivery to the TAL and medullary interstitium.

Similar to characteristics of distal renal tubular acidosis (dRTA), acidotic renal *Ugcg*/*Cst*-deficient mice exhibited impaired NAE. However, classic dRTA is manifested by a high urinary pH even in the presence of systemic acidosis (33, 34). Furthermore, net NH_3 and NH_4^+ fluxes as well as H^+-ATPase–mediated proton secretion across the apical membrane in isolated OMCDs or transepithelial ammonia fluxes in CCDs of acidotic mutant mice were not reduced.

Renal *Ugcg*/*Cst*-deficient mice had higher urinary K^+ at baseline and upon acid loading. Sulfatides have been reported to modulate basolateral Na^+-K^+-ATPase activity in osmoregulatory organs of vertebrates and in the kidney of rodents and pig through different mechanisms (15, 17, 35, 36). Moreover, they have been shown to interact with H^+-K^+-ATPase and influence its activity in the rabbit gastric mucosa (16). However, the slight changes in blood K^+ concentrations at baseline and upon acid loading (*SI Appendix*, Tables S1 and S2) were unlikely to affect renal acid–base handling in mutant mice (37, 38). Concomitantly, ammoniagenesis in isolated proximal tubular segments of double-mutant cortices was similar to controls.

Renal *Cst*- and *Ugcg*/*Cst*-deficient mice had less concentrated urine at baseline and upon HCl loading. Lower ammonium excretion as well as polyuria may be a consequence of a general dysfunction of the countercurrent system. This was excluded as water-deprived renal *Ugcg*/*Cst*-deficient mice exhibited a normal gradient of tissue osmolality. We suggest that polyuria in sulfatide-deficient mice is caused by reduced water reabsorption due to the reactively decreased protein levels of the luminal water channel AQP2 in the CD.

Renal tubular acidosis has been associated with polyuria (33). Increased water intake and diuresis have been suggested as a compensatory regulatory process during metabolic acidosis (39). Decreased water reabsorption by the late distal tubule and CD may reduce NH_3 backflux from lumen to blood by several effects (24). At baseline and during water deprivation, *Ugcg*/*Cst*-deficient mice had normal systemic acid–base parameters. We surmise that, in sulfatide-deficient mice, AQP2 decreased in a compensatory mode at baseline and during the acid load.

Based on our data, we hypothesize that renal sulfatide-deficient mice have an impaired electrostatic ability to keep high interstitial ammonium concentrations in the papilla. Titze et al. (40) have previously demonstrated that increased sodium storage in skin correlates with increased negative charge density provided by sulfated polyanionic glycosaminoglycans in the extracellular matrix of the skin. In analogy, kidney sulfatides may act as counterions of interstitial NH_4^+ neutralizing its positive charge and thereby facilitating its accumulation. We could demonstrate that sulfatation of GalCer is essential for the binding of NH_4^+ (*SI Appendix*, Fig. S9). Renal sulfatide deficiency therefore would result in decreased medullary/papillary interstitial ammonium retention and consequent backrelease into the systemic circulation through the renal vein. Consistent with this interpretation, renal *Ugcg*/*Cst*-deficient mice showed elevated levels of plasma urea, an ammonium metabolite of the liver (41). We did not observe an adaptive increase in renal sulfatide levels in wild-type mice upon acute as well as chronic acid loading. High concentrations of sulfatide in the inner medulla and papilla apparently provide sufficient capacity to cope with the bulk of renal ammonium in response to acidosis.

In summary, we report a renal dysfunction caused by a renal epithelia-specific genetic disruption of sulfatide synthesis. Our data suggest that renal sulfatides may be required to bind ammonium and maintain its high interstitial concentrations in the papilla needed for appropriate urinary ammonium excretion. The impact of sulfatides on renal ammonium excretion is highlighted by the impaired acid stress handling and resulting acidosis in sulfatide-deficient mice.

Materials and Methods

Generation of *Ugcg*$^{f/f}$, *Cst*$^{f/f}$, and *Ugcg*$^{f/f}$ *Cst*$^{f/f}$ Pax8Cre Mice. Mice with disruption of the *Cst* and/or *Ugcg* gene specifically in the kidney were generated by crossing *Cst*-, *Ugcg*-, and *Ugcg*/*Cst*-*floxed* mice, respectively, with mice expressing the Cre-recombinase under control of the Pax8 promoter (20) as described in *SI Appendix*. Generation of mutant mice and all experiments were approved and performed in accordance with federal laws (Regierungspräsidium Karlsruhe, Karlsruhe, Germany).

Acid Loading. Acid loading, blood as well as urine pH, blood gases and electrolytes, titratable acids, bicarbonate, and glutaminase activity were measured as described in *SI Appendix*.

Ammoniagenesis. Ammoniagenesis on isolated proximal tubule segments was measured as described in *SI Appendix*.

GSLs Extraction and Detection. GSLs were extracted according to Sandhoff with modifications (42) and detected by TLC as described in *SI Appendix*.

MALDI Imaging Mass Spectrometry. Mass-spectrometric measurements were performed using Autoflex III MALDI-TOF/TOF instruments (Bruker Daltonics) as described previously (43).

Measurements of Tissue Ammonium and Osmolality. Ammonium content in kidney tissue was measured as previously described (29). Data were initially

calculated as micromoles of ammonium per milligram of protein. Data of two independent experiments were pooled. Renal tissue osmolality measurements were performed as described (44).

Real-Time RT-PCR. Specific mRNA was analyzed using the LightCycler 2.0 System and the LightCyler-FastStart DNA MasterSYBR Green I kit (Roche Diagnostics). Primer sequences are described in *SI Appendix*.

Western Blotting. Proteins were isolated, blotted, and detected as described in *SI Appendix*.

Immunofluorescence. Staining of formalin-fixed kidneys was performed on 3-μm paraffin sections as described in *SI Appendix*.

Physiological in Vitro Studies. Brush border membrane vesicles were assessed by the acridine orange technique as described in ref. 45. Intracellular pH measurements on isolated OMCDs and transepithelial NH_3 permeability measurements on isolated CCDs from acid-loaded mice were performed as described previously (46).

Statistics. Datasets were compared by performing the Mann–Whitney test. Unless otherwise stated, data are expressed as means ± SEM. Differences were considered significant if $P < 0.05$.

ACKNOWLEDGMENTS. We thank S. Kaden, S. Meldner, U. Rothermel, C. Schmidt, T. Sijmonsma, S. Wang, and M. Volz for excellent technical assistance. We thank N. Curthoys and D. Weiner for kindly providing antibodies. H.-J.G. and S.P. were supported by German Research Foundation Grant Sonderforschungsbereich 938, and C.A.W. was supported by Swiss National Science Foundation Grant 31003A_138143. C.H., R.S., and H.-J.G. were supported by a joint grant (Zentrum für Angewandte Forschung–Applied Biomedical Mass Spectrometry) from the Landesstiftung Baden-Württemberg and the Europäischer Fonds für Regionale Entwicklung.

1. Kraut JA, Madias NE (2010) Metabolic acidosis: Pathophysiology, diagnosis and management. *Nat Rev Nephrol* 6(5):274–285.
2. Mulroney SE, Myers AK (2009) Renal physiology. *Netters' Essential Physiology*, ed O'Grady E (Saunders, Philadelphia), 1st Ed, pp 209–240.
3. Wagner CA, Devuyst O, Bourgeois S, Mohebbi N (2009) Regulated acid-base transport in the collecting duct. *Pflugers Arch* 458(1):137–156.
4. Weiner ID, Verlander JW (2011) Role of NH_3 and NH_4^+ transporters in renal acid-base transport. *Am J Physiol Renal Physiol* 300(1):F11–F23.
5. Houillier P, Bourgeois S (2012) More actors in ammonia absorption by the thick ascending limb. *Am J Physiol Renal Physiol* 302(3):F293–F297.
6. Lüllmann-Rauch R, Matzner U, Franken S, Hartmann D, Gieselmann V (2001) Lysosomal sulfoglycolipid storage in the kidneys of mice deficient for arylsulfatase A (ASA) and of double-knockout mice deficient for ASA and galactosylceramide synthase. *Histochem Cell Biol* 116(2):161–169.
7. Tadano-Aritomi K (2003) Structure and function of sulfoglycolipids in the kidney and testis. *Trends Glycosci Glycotechnol* 15(81):15–27.
8. Deshmukh GD, Radin NS, Gattone VH, 2nd, Shayman JA (1994) Abnormalities of glycosphingolipid, sulfatide, and ceramide in the polycystic (cpk/cpk) mouse. *J Lipid Res* 35(9):1611–1618.
9. Kobayashi T, et al. (1993) Sulfolipids and glycolipid sulfotransferase activities in human renal cell carcinoma cells. *Br J Cancer* 67(1):76–80.
10. Ishizuka I (1997) Chemistry and functional distribution of sulfoglycolipids. *Prog Lipid Res* 36(4):245–319.
11. Ogawa D, et al. (2004) Cerebroside sulfotransferase deficiency ameliorates L-selectin-dependent monocyte infiltration in the kidney after ureteral obstruction. *J Biol Chem* 279(3):2085–2090.
12. Nagai K, Tadano-Aritomi K, Niimura Y, Ishizuka I (2008) Higher expression of renal sulfoglycolipids in marine mammals. *Glycoconj J* 25(8):723–726.
13. Niimura Y, Nagai K (2008) Metabolic responses of sulfatide and related glycolipids in Madin-Darby canine kidney (MDCK) cells under osmotic stresses. *Comp Biochem Physiol B Biochem Mol Biol* 149(1):161–167.
14. Karlsson K-A (1971) Lipid pattern and Na^+-K^+-dependent adenosine triphosphatase activity in the salt gland of duck before and after adaption to hypertonic saline. *J Membr Biol* 5(2):169–184.
15. Umeda T, Egawa K, Nagai Y (1976) Enhancement of sulphatide metabolism in the hypertrophied kidney of C3H/He mouse with reference to [Na^+, K^+]-dependent ATPase. *Jpn J Exp Med* 46(1):87–94.
16. Zambrano F, Rojas M (1987) Sulphatide content in a membrane fraction isolated from rabbit gastric mucosal: Its possible role in the enzyme involved in H^+ pumping. *Arch Biochem Biophys* 253(1):87–93.
17. Zalc B, Helwig JJ, Ghandour MS, Sarlieve L (1978) Sulfatide in the kidney: How is this lipid involved in sodium chloride transport? *FEBS Lett* 92(1):92–96.
18. Bosio A, Binczek E, Stoffel W (1996) Functional breakdown of the lipid bilayer of the myelin membrane in central and peripheral nervous system by disrupted galactocerebroside synthesis. *Proc Natl Acad Sci USA* 93(23):13280–13285.
19. Honke K, et al. (2002) Paranodal junction formation and spermatogenesis require sulfoglycolipids. *Proc Natl Acad Sci USA* 99(7):4227–4232.
20. Bouchard M, Souabni A, Busslinger M (2004) Tissue-specific expression of cre recombinase from the Pax8 locus. *Genesis* 38(3):105–109.
21. Yamashita T, et al. (1999) A vital role for glycosphingolipid synthesis during development and differentiation. *Proc Natl Acad Sci USA* 96(16):9142–9147.
22. Tadano-Aritomi K, et al. (2000) Kidney lipids in galactosylceramide synthase-deficient mice. Absence of galactosylsulfatide and compensatory increase in more polar sulfoglycolipids. *J Lipid Res* 41(8):1237–1243.
23. Attmane-Elakeb A, et al. (1998) Stimulation by in vivo and in vitro metabolic acidosis of expression of rBSC-1, the Na^+-K^+($NH4^+$)-$2Cl^-$ cotransporter of the rat medullary thick ascending limb. *J Biol Chem* 273(50):33681–33691.
24. Packer RK, Desai SS, Hornbuckle K, Knepper MA (1991) Role of countercurrent multiplication in renal ammonium handling: Regulation of medullary ammonium accumulation. *J Am Soc Nephrol* 2(1):77–83.
25. Bobulescu IA, Moe OW (2009) Luminal Na^+/H^+ exchange in the proximal tubule. *Pflugers Arch* 458(1):5–21.
26. Seshadri RM, et al. (2006) Changes in subcellular distribution of the ammonia transporter, Rhcg, in response to chronic metabolic acidosis. *Am J Physiol Renal Physiol* 290(6):F1443–F1452.
27. Stehberger PA, et al. (2003) Localization and regulation of the ATP6V0A4 (a4) vacuolar H^+-ATPase subunit defective in an inherited form of distal renal tubular acidosis. *J Am Soc Nephrol* 14(12):3027–3038.
28. Porubsky S, et al. (2012) Globosides but not isoglobosides can impact the development of invariant NKT cells and their interaction with dendritic cells. *J Immunol* 189(6):3007–3017.
29. Bourgeois S, et al. (2010) NHE4 is critical for the renal handling of ammonia in rodents. *J Clin Invest* 120(6):1895–1904.
30. Maalouf NM, Cameron MA, Moe OW, Sakhaee K (2010) Metabolic basis for low urine pH in type 2 diabetes. *Clin J Am Soc Nephrol* 5(7):1277–1281.
31. Sakhaee K (2009) Recent advances in the pathophysiology of nephrolithiasis. *Kidney Int* 75(6):585–595.
32. Bobulescu IA, Dubree M, Zhang J, McLeroy P, Moe OW (2009) Reduction of renal triglyceride accumulation: Effects on proximal tubule Na^+/H^+ exchange and urinary acidification. *Am J Physiol Renal Physiol* 297(5):F1419–F1426.
33. Pereira PC, Miranda DM, Oliveira EA, Silva AC (2009) Molecular pathophysiology of renal tubular acidosis. *Curr Genomics* 10(1):51–59.
34. Karet FE (2002) Inherited distal renal tubular acidosis. *J Am Soc Nephrol* 13(8):2178–2184.
35. Jedlicki A, Zambrano F (1985) Role of sulfatide on phosphoenzyme formation and ouabain binding of the (Na^+ + K^+)ATPase. *Arch Biochem Biophys* 238(2):558–564.
36. Lingwood D, Harauz G, Ballantyne JS (2005) Regulation of fish gill Na^+-K^+-ATPase by selective sulfatide-enriched raft partitioning during seawater adaptation. *J Biol Chem* 280(44):36545–36550.
37. DuBose TD, Jr., Good DW (1991) Effects of chronic hyperkalemia on renal production and proximal tubule transport of ammonium in rats. *Am J Physiol* 260(5 Pt 2):F680–F687.
38. Good DW (1987) Effects of potassium on ammonia transport by medullary thick ascending limb of the rat. *J Clin Invest* 80(5):1358–1365.
39. Nowik M, Kampik NB, Mihailova M, Eladari D, Wagner CA (2010) Induction of metabolic acidosis with ammonium chloride (NH_4Cl) in mice and rats—species differences and technical considerations. *Cell Physiol Biochem* 26(6):1059–1072.
40. Titze J, et al. (2004) Glycosaminoglycan polymerization may enable osmotically inactive Na^+ storage in the skin. *Am J Physiol Heart Circ Physiol* 287(1):H203–H208.
41. Häussinger D, Lamers WH, Moorman AF (1992) Hepatocyte heterogeneity in the metabolism of amino acids and ammonia. *Enzyme* 46(1–3):72–93.
42. Sandhoff R, et al. (2002) Kidney sulfatides in mouse models of inherited glycosphingolipid disorders: Determination by nano-electrospray ionization tandem mass spectrometry. *J Biol Chem* 277(23):20386–20398.
43. Marsching C, Eckhardt M, Gröne HJ, Sandhoff R, Hopf C (2011) Imaging of complex sulfatides SM3 and SB1a in mouse kidney using MALDI-TOF/TOF mass spectrometry. *Anal Bioanal Chem* 401(1):53–64.
44. Herrera M, Garvin JL (2005) A high-salt diet stimulates thick ascending limb eNOS expression by raising medullary osmolality and increasing release of endothelin-1. *Am J Physiol Renal Physiol* 288(1):F58–F64.
45. Honegger KJ, et al. (2006) Regulation of sodium-proton exchanger isoform 3 (NHE3) by PKA and exchange protein directly activated by cAMP (EPAC). *Proc Natl Acad Sci USA* 103(3):803–808.
46. Biver S, et al. (2008) A role for Rhesus factor Rhcg in renal ammonium excretion and male fertility. *Nature* 456(7220):339–343.
47. Jennemann R, et al. (2005) Cell-specific deletion of glucosylceramide synthase in brain leads to severe neural defects after birth. *Proc Natl Acad Sci USA* 102(35):12459–12464.